ADVANCED MATERIALS INTERFACES
www.advmatinterfaces.de

Oligothiophene-Based Phosphonates for Surface Modification of Ultraflat Transparent Conductive Oxides

Melanie Timpel, Marco V. Nardi,* Berthold Wegner, Giovanni Ligorio, Luca Pasquali, Jana Hildebrandt, Michael Pätzel, Stefan Hecht, Hiromichi Ohta, and Norbert Koch*

The self-assembly of electroactive organic molecules on transparent conductive oxides is a versatile strategy to engineer the interfacial energy-level alignment and to enhance charge carrier injection in optoelectronic devices. Via chemical grafting of an aromatic oligothiophene molecule by changing the position of the phosphonic acid anchoring group with respect to the organic moiety (terminal and internal), the direction of the main molecular dipole is changed, i.e., from parallel to perpendicular to the substrate, to study the molecular arrangement and electronic properties at the organic–inorganic interface. It is found that the observed work function increase cannot solely be predicted based on the calculated molecular dipole moment of the oligothiophene-based phosphonates. In addition, charge transfer from the substrate to the molecule has to be taken into account. Molecular assembly and induced electronic changes are analogous for both indium-tin oxide (ITO) and zinc oxide (ZnO), demonstrating the generality of the approach and highlighting the direct correlation between molecular coverage and electronic effects.

1. Introduction

Hybrid inorganic/organic systems for optoelectronic applications require organic molecules that respond to the demand for efficient electronic coupling with the inorganic components, allowing mobile charge carriers to move across the interface. In the field of organic electronics, typical organic semiconductors consist of acene- or thiophene-based building blocks, such as conjugated oligomers and polymers.[1,2] When such organic molecules are equipped with a phosphonic acid (PA) group, they can be covalently linked to inorganic electrical contacts, such as transparent conductive oxides, e.g., indium-tin oxide (ITO)[3] and zinc oxide (ZnO).[4,5] These phosphonate monolayers render the oxide surface more stable over time in ambient conditions by effectively

Dr. M. Timpel, Dr. M. V. Nardi, Dr. B. Wegner, Dr. G. Ligorio, Prof. N. Koch
Institut für Physik & IRIS Adlershof
Humboldt-Universität zu Berlin
Brook-Taylor-Str. 6, Berlin 12489, Germany
E-mail: melanie.timpel@unitn.it; marcovittorio.nardi@unitn.it

Dr. M. Timpel, Dr. M. V. Nardi
Istituto dei Materiali per l'Elettronica ed il Magnetismo
IMEM-CNR
Sezione di Trento
Via alla Cascata 56/C (Povo), Trento 38123, Italy

Prof. L. Pasquali
IOM-CNR Institute
Area Science Park
SS 14 Km, 163.5, Basovizza, Trieste 34149, Italy

Prof. L. Pasquali
Engineering Department
"E. Ferrari"
University of Modena e Reggio Emilia
Via Vivarelli 10, Modena 41125, Italy

The ORCID identification number(s) for the author(s) of this article can be found under https://doi.org/10.1002/admi.201902114.

DOI: 10.1002/admi.201902114

Prof. L. Pasquali
Department of Physics
University of Johannesburg
PO Box 524, Auckland Park 2006, South Africa

J. Hildebrandt, Dr. M. Pätzel, Prof. S. Hecht
Institut für Chemie
Humboldt-Universität zu Berlin
Brook-Taylor-Str. 2, Berlin 12489, Germany

Prof. S. Hecht
DWI – Leibniz Institut für Interaktive Materialien e.V.
RWTH Aachen University
Forckenbeckstraße 50, Aachen 52056, Germany

Prof. S. Hecht
Institut für Technische und Makromolekulare Chemie
RWTH Aachen University
Worringerweg 2, Aachen 52074, Germany

Prof. H. Ohta
Research Institute for Electronic Science
Hokkaido University
N20W10, Sapporo 001-0020, Japan

Prof. N. Koch
Helmholtz-Zentrum Berlin für Materialien und Energie GmbH
Albert-Einstein-Str. 16, Berlin 12489, Germany

Prof. N. Koch
Jiangsu Key Laboratory for Carbon Based Functional Materials and Devices and Institute of Functional Nano and Soft Materials (FUNSOM)
Soochow University
199 Ren-Ai Road, Suzhou 215123, China

passivating the surface. Furthermore, it has been shown that such PA monolayers can increase the charge injection efficiently across the inorganic/organic interface, and thus, improve the performance of ITO-based[6–9] and ZnO-based[10,11] optoelectronic devices. Thus, the PA molecules can be employed to functionalize the electrode in an arrangement of a self-assembled monolayer (SAM) that effectively forms a (non) resonant tunneling barrier for charges from/to the organic counterpart in optoelectronic devices.[12]

Besides interfacial engineering of the electronic properties, the phosphonate monolayers can potentially be used as organic coating to facilitate the formation of overlayers of conjugated polymers as active material, e.g., by subsequent on-surface polymerization methods.[13–15] In this context, one has to consider, first, that phosphonate monolayers enable the molecules in the organic overlayer to adopt a different arrangement relative to that on the unmodified substrate,[16] and second, that the arrangement critically depends on the morphology and polarity of the phosphonate monolayer.[17] Adjusting the surface energy for proper wetting and optimal orientation of the active materials at the interface may have a strong effect on optoelectronic device performance.[3]

In the present study, we used conjugated oligomers, namely quinquethiophene (T5) modified with a PA group in terminal (tP) and internal (iP) position (see **Figure 1**) to covalently attach them to ultraflat ITO and ZnO surfaces. The latter aspect is important as it facilitates an improved analysis of molecular order and its effect on SAM properties, while rougher variants of these substrate materials would have adverse impact. The variation of the PA position on the thiophene moiety helped us to control the orientation and surface coverage of the conjugated molecules on the inorganic surfaces, and thus, to tune the electronic properties and molecule orientation. The findings of this study will help to control the arrangement of virtually any possible organic overlayer, since this will critically depend on the arrangement of the PA interlayer.

We characterized the electronic properties and molecular coverage of the T5-tP/iP-modified ITO and ZnO surfaces collecting valence band (ultraviolet photoelectron spectroscopy, UPS) and core level (X-ray photoelectron spectroscopy, XPS) spectra, and determined the orientation of the molecules within the T5-tP/iP monolayers relative to the metal oxide surfaces via X-ray absorption spectroscopy (XAS) measurements. The UPS measurements were further supported by density functional theory (DFT) calculations in order to unambiguously identify the contribution of the phosphonate to the valence band spectra of the T5-tP/iP-modified surfaces.

2. Results

The quality and surface morphology of the bare ultraflat ITO and ZnO(0001)–Zn substrates were investigated by atomic force microscopy (AFM) before surface modification, see **Figure 2**. The intermittent contact mode AFM height image of the ITO film (Figure 2a) reveals flat terraces with widths of up to 150 nm and a roughness (root-mean-square, rms) of ≈0.1 nm, in good agreement with previous reports.[18,19] Likewise, the corresponding cross-section analysis (lower panel in Figure 2a) yields terrace step heights that are in the order of two adjacent ITO planes (0.3 nm).[18] The ZnO surface in Figure 2b shows the typical terrace structure as previously observed,[5] with terrace step heights in the order of ≈1 nm (lower panel in Figure 2b), indicating multiple (4× and more) Zn–O layer step heights. Overall, the ZnO terraces exhibit a smooth and featureless surface morphology with a roughness of ≈0.15 nm.

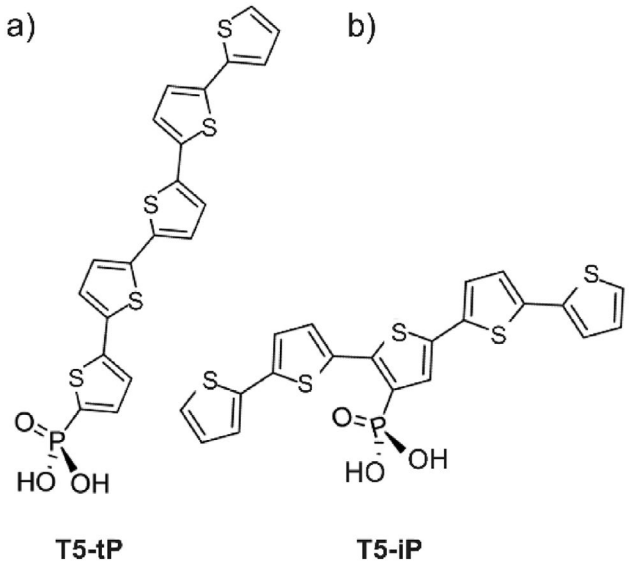

Figure 1. Molecular structure of the phosphonic acids (PAs) used for modification of the ITO/ZnO surfaces: quinquethiophene with a) terminal (T5-tP) and b) internal (T5-iP) phosphonic acid substitution.

After surface modification, the density of molecules present in the T5-tP/iP monolayers on both ITO and ZnO were evaluated by XPS measurements of molecule- (S 2p, P 2p) and substrate-specific (In 3d and Zn 3s/Zn 2p, respectively) core levels. The analysis of the molecules' binding to both metal oxide surfaces, as evaluated by O 1s core level fitting analysis and described in detail in ref. [5], is shown in Figure S1 (Supporting Information). Briefly, for fitting we used binding energy positions corresponding to two binding modes, namely bidentate and tridentate binding, which were previously calculated to be stable configurations for PA adsorption on the ZnO(0001)–Zn surface.[20] In agreement with our previous findings of PA-modified ZnO(0001)–Zn surfaces,[5,17] the fitting results point toward a mixture of bidentate and tridentate modes for both metal oxide surfaces (≈60% bidentate), with a slightly lower fraction of bidentate binding for T5-iP on ZnO (≈50% bidentate).

Figure 3 summarizes the fitting analysis of the S 2p, P 2p (Zn 3s + P 2p) and In 3d (Zn 2p) core level regions of the T5-tP/iP-modified ITO (ZnO) surface. As can be derived from the S 2p (Figure 3a) and P 2p (Figure 3b) core level intensities, the T5-tP-modified ITO exhibits approximately double molecular coverage as compared to the T5-iP-modified ITO surface. The In $3d_{5/2}$ peak of both PA-modified ITO surfaces (Figure 3c), and the pristine one, was found at a constant binding energy (BE) of 444.6 eV BE, indicating negligible band bending with respect to the bare surface.

Similar to the results obtained on ITO, the T5-tP-modified ZnO shows approximately double molecular coverage than the

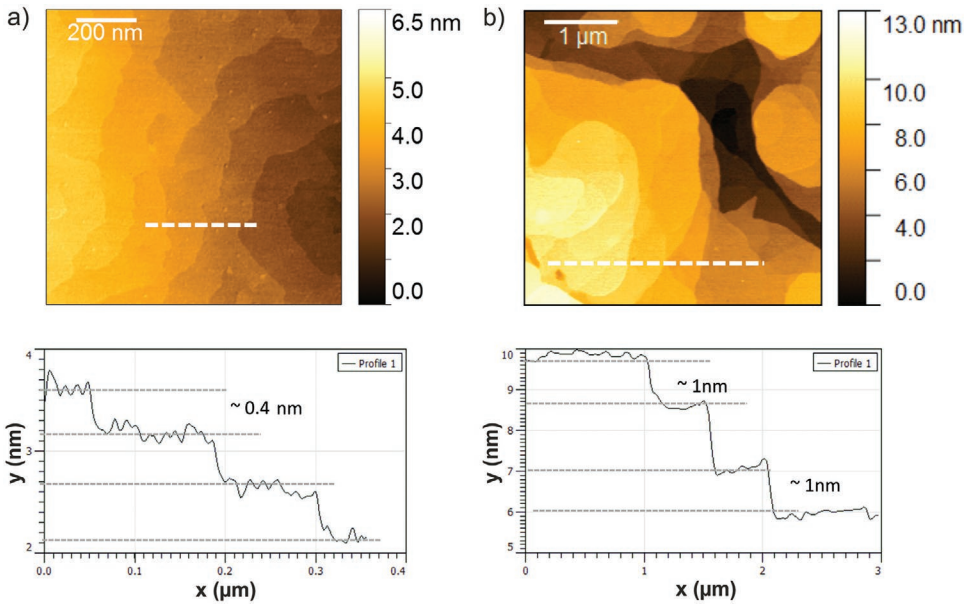

Figure 2. AFM height images of the ultraflat a) ITO and b) ZnO surface; lower panels show cross-sections along the dotted lines in (a) and (b), respectively.

T5-iP-modified ZnO, as obvious from the S 2p and P 2p + Zn 3s core level regions (see Figure 3d,e). In analogy with the ITO surface, both Zn 3s (Figure 3d) and Zn 2p (Figure 3e) core levels do not show any shift after surface modification, indicating the absence of adsorption-induced band bending in ZnO.

The UV/Vis absorption spectra of T5-iP-modified ITO in combination with the spectra of T5-iP molecules in solution (see Figure S2 in the Supporting Information) can be used to estimate the surface coverage based on the Beer–Lambert law.[21] The T5-iP absorbs in the UV/Vis region and its transition dipole moment μ_T is polarized essentially parallel to the long molecular axis, and thus approximately parallel to the substrate surface (see detailed calculations in the Supporting Information), which can be expected from the molecular geometry (see Figure 1b). The estimation via UV/Vis gives a molecular coverage σ of the T5-iP-modified ITO of 0.5 molecules nm^{-2}, which is in the same order of magnitude as our previous estimation based on work function (WF) modification and Helmholtz equation for alkyl- and arene-based PA molecules on ZnO.[5] Based on the molecular coverage σ of the T5-iP-modified ITO (as determined via UV/Vis), and considering the XPS signals stemming from S 2p and P 2p reported in Figure 3, the molecular coverage of T5-tP-modified ITO amounts to about 2.0 molecule nm^{-2}, which is in agreement with previously reported values for similar PA-modified ITO surfaces.[3]

Figure 4 shows the XAS spectra for the T5-tP-modified ITO (Figure 4a) and ZnO (Figure 4b) surfaces collected at five different ψ_C angles of the scattering chamber spanning from 0° to 90°, corresponding to varying from s- to p- polarization geometries (see ref. [23] for details). On both substrates, the T5-tP monolayer, i.e., the one with the PA group in terminal position (Figure 1a), clearly exhibits an angular dependence that can be associated to a preferential orientation with respect to the substrate surface, considering that the PA group in terminal position binds to the metal oxide surface. A fit of the Stöhr equation to the experiment, assuming on average an in-plane isotropic domain arrangement[22,23] and considering the area of the transition-peak located at 286.0 eV (the molecule's transition dipole moment associated with this peak is shown in Figure S5a in the Supporting Information) results in a tilt angle of the long molecular axis with respect to the substrate normal of 23° and 24°, respectively. Notably, the corresponding T5-iP monolayers, i.e., those with the PA group in internal position (Figure 1b), show no preferential orientation on both metal oxide surfaces (see Figure S5b,c in the Supporting Information).

The surface electronic properties of the ITO and ZnO substrates before (i.e., unmodified) and after T5-iP/tP modification were characterized by UPS (see **Figure 5**). As can be seen for the ITO (upper panel) and ZnO surface (lower panel) in Figure 5a, the T5-tP monolayer (blue line) increases the WF of ITO (ZnO) by +1.0 eV (+1.15 eV). In contrast to that, the T5-iP monolayer (red line) does not result in any WF change on both surfaces. Figure 5b displays the valence region close to the Fermi level E_F of the unmodified and T5-tP/iP-modified ITO (ZnO) surface, respectively. Molecule-related emission features (labeled as loc-π, H^{-1} and H in Figure 5b) can be readily assigned to the highest occupied molecular orbital (HOMO) level of the T5-tP (blue line) and T5-iP (red line) molecules [labeled H], the HOMO-1 level [labeled H^{-1}], and the five almost degenerate localized π-orbital levels [labeled loc-π]. It is noteworthy that the HOMO and HOMO-1 features of the T5-tP-modified surface are well resolved in energy (labeled as H^{-1} and H), which is correctly reproduced by the projected density of states (DOS) calculated at the DFT level of the T5-tP free molecule (see Figure 5c, upper panel), whereas T5-iP shows comparably merged HOMO and HOMO-1 features (labeled as H^{-1} + H). This finding is in agreement with the calculated DOS of T5-iP in Figure 5c (lower panel). Additionally, the valence band features measured on ITO (Figure 5b, upper panel) are

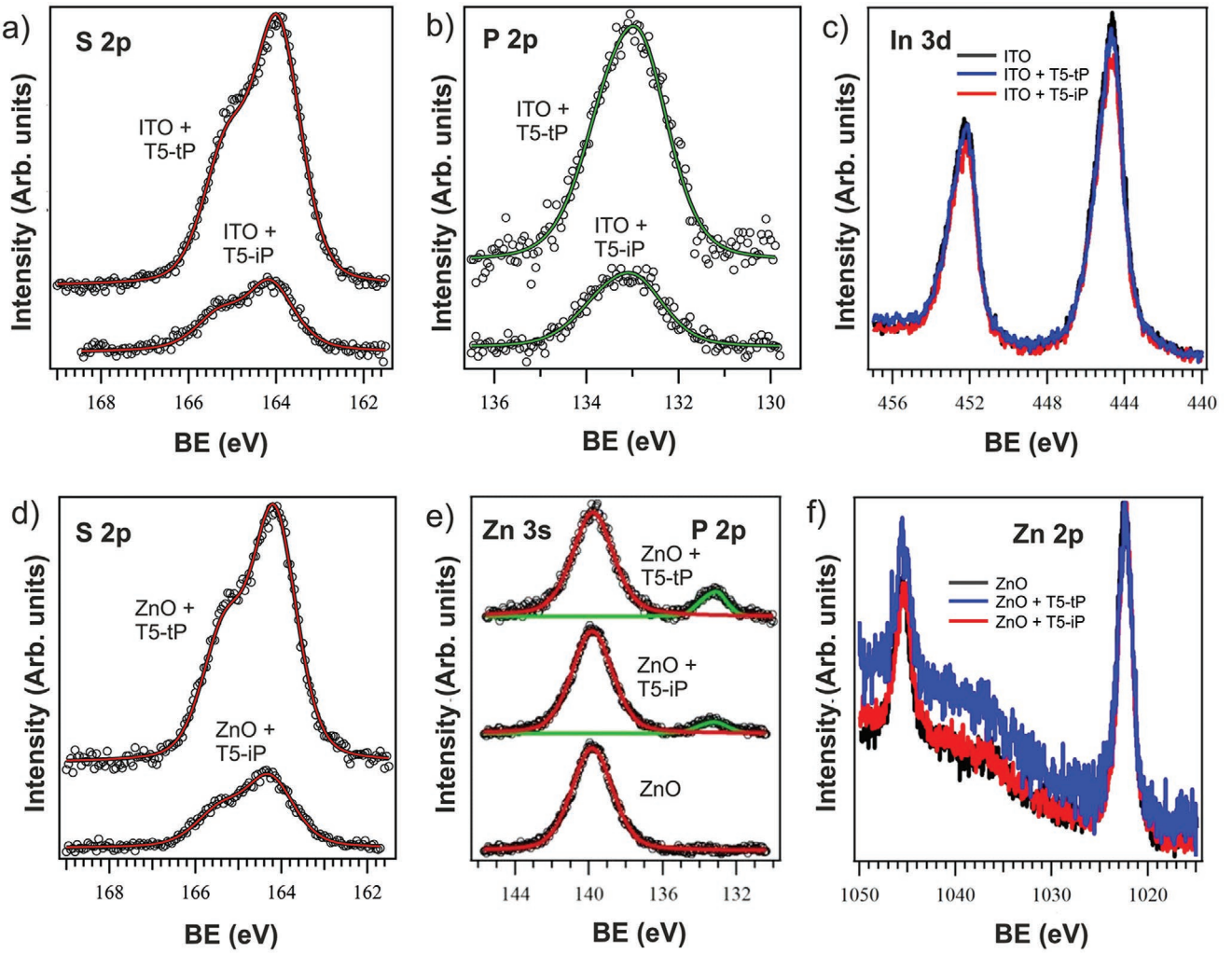

Figure 3. XPS core level spectra (background subtracted) of the a) S 2p, b) P 2p, and c) In 3d region of the T5-iP- and T5-tP-modified ITO surface as indicated in the figure; d) S 2p, e) Zn 3s + P 2p, and f) Zn 2p region of the T5-ip-modified and T5-tp-modified ZnO surface as indicated in the figure.

well reproduced by the calculated DOS for both T5-tP and T5-iP, supporting the idea of a good molecular ordering at the surface.

Accordingly, the valence region UPS spectrum of T5-tP/iP-modified ZnO (see Figure 5b, lower panel) is comparable to that of T5-tP/iP-modified ITO, except that the fine structure of the T5-tP's HOMO and HOMO-1 is less pronounced. Overall, these findings point toward an analogous behavior of the two molecules on both ultraflat metal oxide surfaces.

3. Discussion

To elucidate the effects of the surface modification of ITO and ZnO on the frontier interfacial energy levels, we schematically summarize the energy-level alignment of unmodified and corresponding T5-tP/iP-modified ITO/ZnO surfaces in **Figure 6**. Two remarkable differences regarding T5-tP and T5-iP (analogous for both ITO and ZnO substrates) are found. First, the WF increased only in the case of T5-tP-modified surfaces (by ≈1 eV), whereas for the T5-iP-modified surfaces no WF change could be detected. In general, the total work function change $\Delta\phi$ can be expressed as a combination of three conceptually independent components[3,24–29]

$$\Delta\phi = \Delta V_{\text{mol}} + \Delta V_{\text{int.dip}} + \Delta V_{\text{geom.rel}} \quad (1)$$

Here, ΔV_{mol} is the component of the intrinsic dipole moment of the molecule perpendicular to the substrate surface, which induces an electrostatic potential energy change across the adsorbed monolayer. Usually this component corresponds to the main contribution of $\Delta\phi$;[3] $\Delta V_{\text{geom.rel}}$ is the geometric rearrangement of the substrate, and $\Delta V_{\text{int.dip}}$ is the electronic reorganization resulting from the PA adsorption on the substrate.

For T5-tP/iP free molecules, the calculated intrinsic dipole moment is oriented away from the PA group, i.e., the PA group is negative, giving a dipole moment of 2.5 and 1.6 D for T5-tP and T5-iP, respectively. Thus, one would expect a work function decrease for the T5-tP/iP-modified ITO/ZnO surfaces. Indeed, previous studies[6] reported a slight WF decrease of T4-tP-modified ITO (by 0.3 eV, as measured via Kelvin probe). This contrasts with the experimentally observed increase of the WF

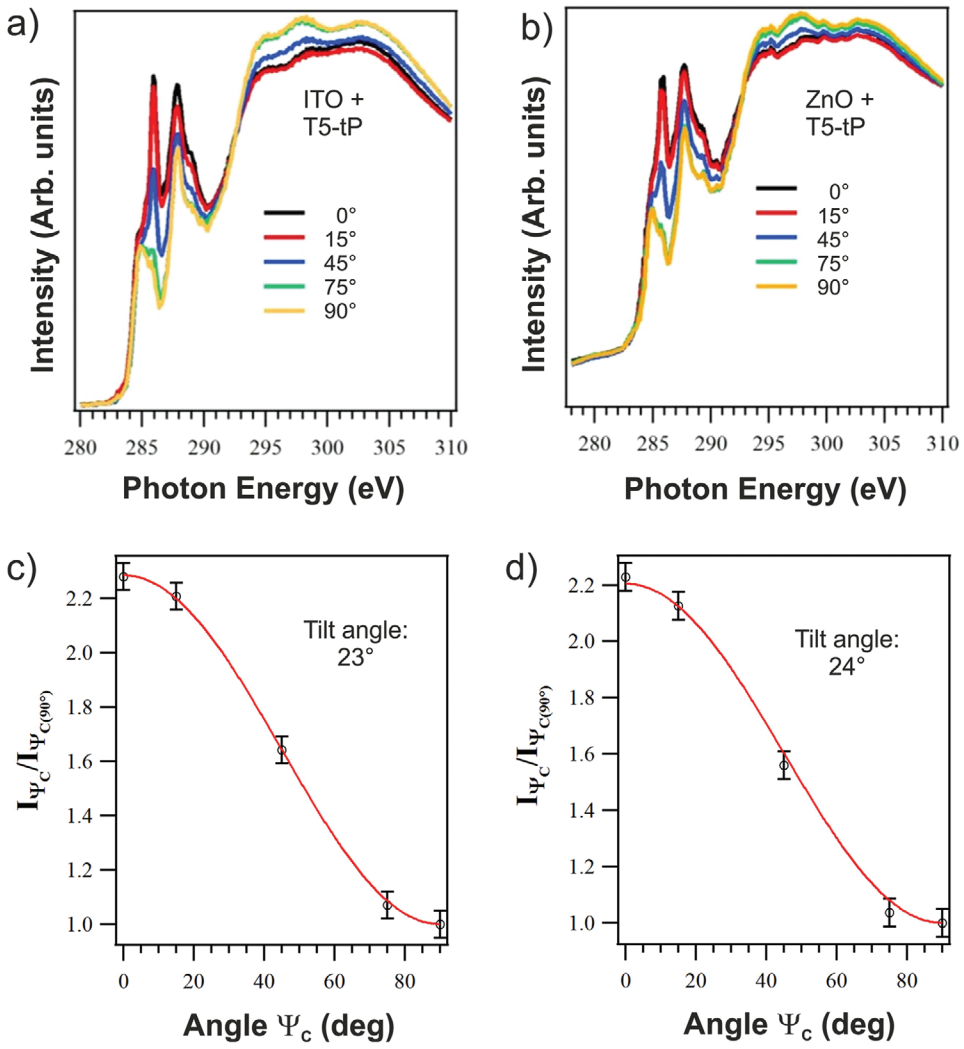

Figure 4. a,b) Experimental C K-edge XAS spectra of the T5-tP-modified a) ITO and b) ZnO surface; c,d) Plots of the relative σ^*- and π^*-orbital intensities as a function of the scattering geometry Ψ_C corresponding to the polarization varying from s to p. The solid curve corresponds to the best fit of the intensity evolution for T5-tP-modified c) ITO and d) ZnO surface with molecule tilt angle of 23° and 24°, respectively, referred to the surface normal.

for the T5-tP case. The effect of geometry relaxation ($\Delta V_{\text{geom.rel}}$) of the ITO/ZnO surfaces is assumed to be negligible, since the WF modification was found to be the same for the two substrates.

The effect of bonding on the WF modification ($\Delta V_{\text{int.dip}}$) may be estimated qualitatively by bonding two In atoms to the two -OH groups of the PA (PO_3H_2) moiety (simulating the bonding with the ITO surface). Mulliken population analysis in this case indicates that electron density migrates from the In atoms to the oxygen atoms of the PA. This charge transfer renders the In atom more positive and the oxygen atoms more negative (i.e., 25–30% more negative with respect to the free molecules), thus contributing to $\Delta\phi$.

Therefore, electron transfer from the substrate to the molecule can justify the increase of the WF experimentally obtained for the densely packed and preferentially oriented T5-tP monolayers on ITO and ZnO. In the case of the T5-iP monolayers, where no WF change was measured, the phosphonate bonds of the T5-iP molecules are most probably highly strained as the quinquethiophene moiety has to tilt on the ITO/ZnO surface. Thus, one can expect i) a different charge redistribution upon bond formation of sterically hindered T5-iP molecules, and ii) more tilted (i.e., less effective) dipole compared to T5-tP. Furthermore, iii) the PA coverage is significantly lower (≈75%, see Figure 3a,b), which does not allow for the formation of a dense dipole layer, and therefore the WF increase might occur only locally (i.e., the dipole field decays laterally on the length scale of the molecules)[30,31] and between two molecules the WF converges to that of the substrate. Accordingly, the much less dense dipole layer of T5-iP experimentally results in a WF that converges to that of ITO/ZnO; an effect related to UPS analysis of heterogeneous surfaces, as recently reported by Schulz et al.[32] This also implies that in the case of T5-iP-modified surfaces, the extracted ionization energy (IE) value (as estimated via experimentally determined WF values) has no practical meaning, while the BE values of valence levels are correctly obtained. In fact, we expect a higher IE for the molecule with parallel orientation

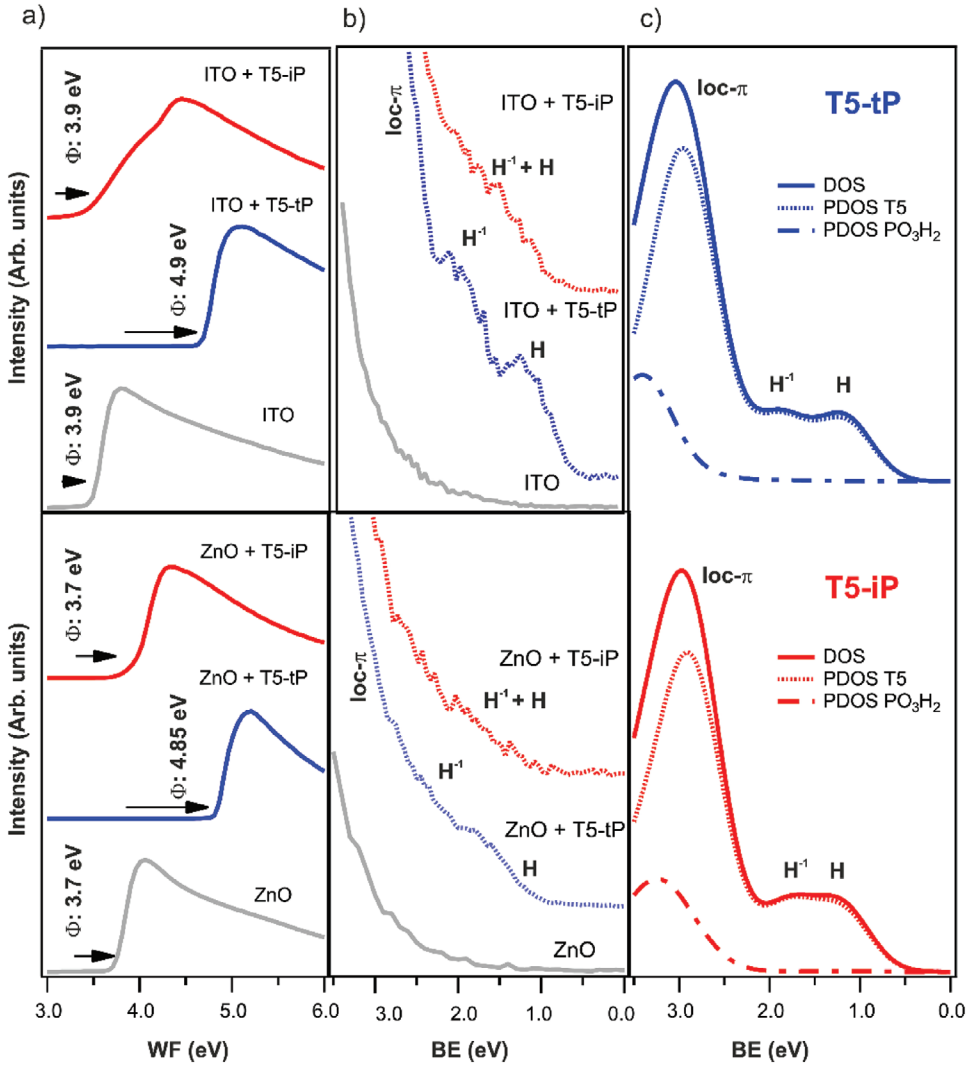

Figure 5. a) SECO and b) valence band region UPS spectra (the near E_F region) of the unmodified, T5-iP-modified, and T5-tP-modified ITO (upper panel) and ZnO (lower panel) surface as indicated in the figure; c) calculated total and partial density of states (DOS) of both molecules.

to the substrate surface (i.e., T5-ip) compared to more vertically arranged one (i.e., T5-tp), since the "flat-lying" orientation of thiophenes results in higher IE values (of more than 0.5 eV) due to collective electrostatic effects.[33] The higher BE of the HOMO of T5-ip (with respect to the Fermi level) compared to that of the "upright-standing" T5-tp (by ≈0.2 eV, see Figure 6) is in agreement with an expected higher IE for the T5-ip molecule. Based on the molecular structure of T5-ip and the relatively low coverage, we do not expect crystalline packing in the SAM. In contrast, the PA group in terminal position (T5-tP) allows for π–π interaction of its thiophene rings in the T5-tP monolayer, facilitating the ordered arrangement of the T5-tP molecules and increasing the overall surface coverage.

4. Conclusion

Two aromatic oligothiophene-based phosphonates with the phosphonic acid anchoring group in internal and terminal position were used to form self-assembled monolayers on ultra-flat ITO and Zn-terminated ZnO surfaces in order to engineer the energy-level alignment at the hybrid inorganic/organic semiconductor interface. By combining surface photoelectron (XPS/UPS) and XAS spectroscopy studies with DFT calculations, we observe an analogous behavior for both ITO and ZnO in terms of bonding, molecular coverage, and arrangement of the phosphonates with respect to the surfaces.

We find that the interface dipole $\Delta V_{\text{int.dip}}$, due to charge redistribution at the interface between the adsorbed monolayer and the surface, is the main contribution for the observed work function increase for T5-tP-modified surfaces, and not the permanent dipole moment ΔV_{mol} of the oligothiophene moiety attached to the anchoring group. This is in contrast with common understanding that (in a first approximation) the WF modification can be estimated by the intrinsic dipole moment of the molecule. Furthermore, the apparent ionization energy values of the two molecules in the covalently bound SAM were found to be strongly impacted by the interfacial

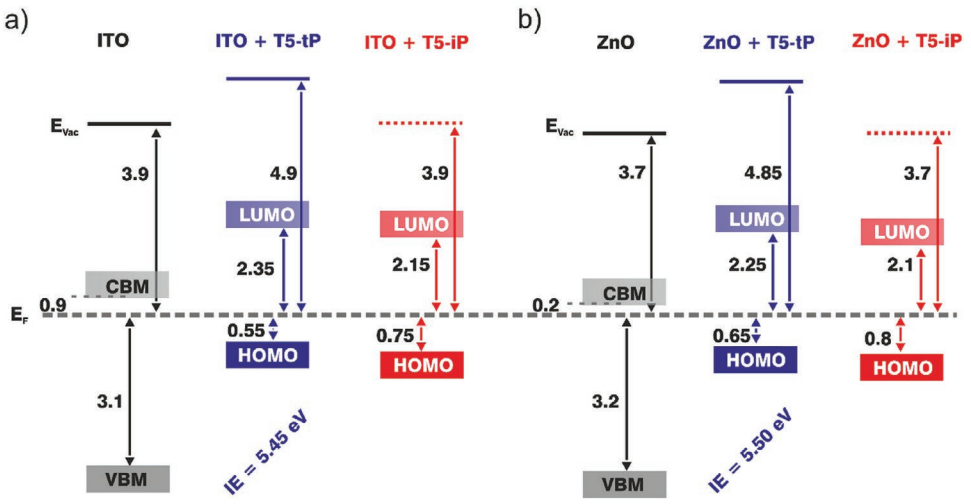

Figure 6. Energy-level diagrams of the unmodified a) ITO and b) ZnO surface (black), and the corresponding T5-tP- (blue) and T5-iP-modified (red) surfaces. The energetic positions of the E_{vac} and HOMO (VBM) relative to E_F were determined by UPS measurements. The CBM onsets for ITO and ZnO were estimated considering their electronic band gaps (ITO: 4.0 eV,[25] ZnO : 3.4 eV[26,27]). Since the behavior of the band bending at the interfaces is unknown, a flat band condition is assumed. The HOMO–LUMO gaps of T5-tP/iP were estimated with an optical gap of 2.5 eV (obtained via UV/Vis spectroscopy, see Figure S2d in the Supporting Information) and assuming an exciton binding energy similar to that of sexithiophene (α-6T), namely 0.4 eV.[28,29]

dipole layer density. While for T5-tp the high packing density has the expected effect on the WF and thus IE value, the much lower packing density determined for T5-ip results in a much reduced impact on sample WF and thus IE value. Since the WF change induced by molecular dipoles depends on the surface coverage,[31] controlling the surface coverage provides a potential means for further fine-tuning of the work function. Furthermore, also mixing of two different dipolar species can be applied for work function fine-tuning, as exemplarily shown in ref. [34]. In device engineering approaches, often published individual material parameters, such as ionization energy, electron affinity, and intrinsic molecular dipole moment, are used as guide for material selection. Our findings, however, emphasize the need to carefully understand the specific details of the interface formed, where also molecular orientation and packing density in a SAM must be considered to reliably control the energy-level alignment.

5. Experimental Section

Synthesis of T5-tp and T5-ip: Quinquethiophene phosphonic acids were prepared in Stille crosscoupling reactions of di- and terthiophene iodides with suitable functionalized thiophenes, bearing a diethylphosphonate moiety. Final hydrolysis of the intermediately formed phosphonates afforded target compounds T5-tP and T5-iP as orange solids, sparingly soluble in organic solvents.[35,36] More details about the synthesis and characterization can be found in the Supporting Information. Figure 1 shows the molecular structure of the quinquethiophene derivatives, carrying a phosphonic acid functional group either at the terminal or internal position (T5-tP/iP).

Ultraflat Substrates: Ultraflat ITO films were grown by pulsed laser deposition on (111) yttria-stabilized zirconia surface, as described previously.[18,19] Smooth, atomically flat ZnO surfaces were obtained by annealing single-crystal ZnO(0001)–Zn substrates (CrysTec, Germany) in a tube furnace (Gero, SR 40-200) under ambient atmosphere at 1000 °C.[5,17]

Ultraflat Substrates—Monolayer Preparation: To prepare the monolayers on the metal oxide surfaces for surface modification, a three-cycle wet-chemical preparation method was adopted from our earlier studies.[5,17] Briefly, each cycle corresponds to the following preparation steps: a) immersion of the substrates in a 0.1×10^{-3} M tetrahydrofuran (THF) solution of the corresponding PA for 2 h; b) annealing on a hot plate under ambient atmosphere at 140 °C for 1/2 h; c) sonication in THF for 15 min.

Atomic Force Microscopy: AFM measurements of the unmodified ITO and ZnO surfaces were performed in intermittent contact mode and under ambient conditions using a NanoWizard 3 (JPK Instruments AG, Germany) instrument. Height and phase images were recorded using aluminium-coated silicon cantilevers (Olympus Corporation, Japan) with a typical resonant frequency of 75 kHz and a spring constant of about 2 N m^{-1}. To compensate for thermal drifts and sample inclination, first-order line subtraction and plane correction were applied to the images.

X-Ray Photoelectron Spectroscopy: The UPS and XPS analysis was carried out using a He discharge lamp (HeI $\alpha = 21.2$ eV) and an Al Kα radiation source (1486.7 eV), respectively, and a hemispherical energy analyzer (Omicron EA125) with an overall energy resolution of <120 meV. All UPS spectra were taken with a filter that lowers the photon flux by at least one order of magnitude and removes the He satellites (HeI $\beta = 23.09$ eV, HeI $\gamma = 23.75$ eV). The sample work function was determined from the secondary electron cutoff (SECO) under an applied sample bias of –10 V. All spectra were recorded at room temperature and normal emission.

X-Ray Absorption Spectroscopy: XAS data were collected at the BEAR endstation (BL8.1L), at the left exit of the 8.1 bending magnet of the ELETTRA synchrotron facility in Trieste (Italy).[37,38] All XAS spectra were collected in total electron yield (TEY) mode at the C K-edge and normalized to the incident photon flux and to the clean substrate signal. The spectral energy was calibrated by referring to CO_2 C 1s–π^* transitions. The details of the geometrical setup at the BEAR endstation to acquire XAS at different angles ψ_C are described elsewhere.[5]

Density Functional Theory calculations: The calculations of the free-molecules T5-tP and T5-iP equilibrium geometry, DOS and dipole moments μ were carried out through DFT by using the StoBe code.[39] All-electron triple-valence plus polarization (TZVP) atomic Gaussian basis sets and gradient-corrected RPBE-PBE revised Perdew-Burke-Ernerhof exchange-correlation functional were used. The calculated total and partial density of states (DOS and PDOS) were convoluted with Gaussians of 0.6 eV FWHM before comparison with the experiment.

Supporting Information

Supporting Information is available from the Wiley Online Library or from the author.

Acknowledgements

M.T. and M.V.N. contributed equally to this work. The authors thank Jürgen P. Rabe for granting access to AFM. This work was financially supported by the Deutsche Forschungsgemeinschaft (DFG) – Projektnummer 182087777 – SFB 951, the European Commission FP7 Project HYMEC (Grant No. 263073), and the Helmholtz-Energie-Allianz "Hybrid-Photovoltaik". This research was also supported by Grants-in-Aid for Scientific Research A (17H01314) and Innovative Areas (19H05791) from the JSPS.

Conflict of Interest

The authors declare no conflict of interest.

Keywords

Indium-tin oxide, phosphonic acid, photoelectron spectroscopy, self-assembled monolayer, zinc oxide

Received: December 15, 2019
Revised: March 13, 2020
Published online: May 4, 2020

[1] A. J. Heeger, *Angew. Chem., Int. Ed.* **2001**, *40*, 2591.
[2] G. Witte, C. Wöll, *J. Mater. Res.* **2004**, *19*, 1889.
[3] S. A. Paniagua, A. J. Giordano, O. L. Smith, S. Barlow, H. Li, N. R. Armstrong, J. E. Pemberton, J.-L. Brédas, D. Ginger, S. R. Marder, *Chem. Rev.* **2016**, *116*, 7117.
[4] P. J. Hotchkiss, M. Malicki, A. J. Giordano, N. R. Armstrong, S. R. Marder, *J. Mater. Chem.* **2011**, *21*, 3107.
[5] M. Timpel, M. V Nardi, S. Krause, G. Ligorio, C. Christodoulou, L. Pasquali, A. Giglia, J. Frisch, B. Wegner, P. Moras, N. Koch, *Chem. Mater.* **2014**, *26*, 5042.
[6] E. L. Hanson, J. Guo, N. Koch, J. Schwartz, S. L. Bernasek, *J. Am. Chem. Soc.* **2005**, *127*, 10058.
[7] J. Guo, N. Koch, S. L. Bernasek, J. Schwartz, *Chem. Phys. Lett.* **2006**, *426*, 370.
[8] J. A. Bardecker, H. Ma, T. Kim, F. Huang, M. S. Liu, Y.-J. Cheng, G. Ting, A. K.-Y. Jen, *Adv. Funct. Mater.* **2008**, *18*, 3964.
[9] K. M. Knesting, H. Ju, C. W. Schlenker, A. J. Giordano, A. Garcia, O. L. Smith, D. C. Olson, S. R. Marder, D. S. Ginger, *J. Phys. Chem. Lett.* **2013**, *4*, 4038.
[10] A. L. Briseno, T. W. Holcombe, A. I. Boukai, E. C. Garnett, S. W. Shelton, J. J. M. Fréchet, P. Yang, *Nano Lett.* **2010**, *10*, 334.
[11] I. Lange, S. Reiter, M. Pätzel, A. Zykov, A. Nefedov, J. Hildebrandt, S. Hecht, S. Kowarik, C. Wöll, G. Heimel, D. Neher, *Adv. Funct. Mater.* **2014**, *24*, 7014.
[12] T. Mosciatti, M. G. del Rosso, M. Herder, J. Frisch, N. Koch, S. Hecht, E. Orgiu, P. Samorì, *Adv. Mater.* **2016**, *28*, 6606.
[13] N. Doubina, S. A. Paniagua, A. V. Soldatova, A. K. Y. Jen, S. R. Marder, C. K. Luscombe, *Macromolecules* **2011**, *44*, 512.
[14] N. Doubina, J. L. Jenkins, S. A. Paniagua, K. A. Mazzio, G. A. MacDonald, A. K. Y. Jen, N. R. Armstrong, S. R. Marder, C. K. Luscombe, *Langmuir* **2012**, *28*, 1900.
[15] S. A. Paniagua, Y. Kim, K. Henry, R. Kumar, J. W. Perry, S. R. Marder, *ACS Appl. Mater. Interfaces* **2014**, *6*, 3477.
[16] J. Gantz, D. Placencia, A. Giordano, S. R. Marder, N. R. Armstrong, *J. Phys. Chem. C* **2013**, *117*, 1205.
[17] M. Timpel, M. V. Nardi, G. Ligorio, B. Wegner, M. Pätzel, B. Kobin, S. Hecht, N. Koch, *ACS Appl. Mater. Interfaces* **2015**, *7*, 11900.
[18] H. Ohta, M. Orita, M. Hirano, H. Hosono, *J. Appl. Phys.* **2002**, *91*, 3547.
[19] H. Ohta, T. Kambayashi, M. Hirano, H. Hoshi, K. Ishikawa, H. Takezoe, H. Hosono, *Adv. Mater.* **2003**, *15*, 1258.
[20] C. Wood, H. Li, P. Winget, J.-L. Brédas, *J. Phys. Chem. C* **2012**, *116*, 19125.
[21] D. F. Swinehart, *J. Chem. Educ.* **1962**, *39*, 333.
[22] J. Stöhr, *NEXAFS Spectroscopy*, Springer, Berlin, Germany **1992**.
[23] L. N. Serkovic Loli, H. Hamoudi, J. E. Gayone, M. L. Martiarena, E. A. Sanchez, O. Grizzi, L. Pasquali, S. Nannarone, B. P. Doyle, C. Dablemont, V. A. Esaulov, *J. Phys. Chem. C* **2009**, *113*, 17866.
[24] G. Heimel, L. Romaner, J.-L. Brédas, E. Zojer, *Phys. Rev. Lett.* **2006**, *96*, 2.
[25] I. Hamberg, C. G. Granqvist, *J. Appl. Phys.* **1986**, *60*, R123.
[26] D. Vogel, P. Kriiger, J. Pollmann, *Phys. Rev. B* **1995**, *52*, R14316.
[27] V. Srikant, D. R. Clarke, *J. Appl. Phys.* **1998**, *83*, 5447.
[28] L. M. Blinov, S. P. Palto, G. Ruani, C. Taliani, A. A. Tevosov, S. G. Yudin, R. Zamboni, *Chem. Phys. Lett.* **1995**, *232*, 401.
[29] I. G. Hill, A. Kahn, Z. G. Soos, R. A. Pascal Jr., *Chem. Phys. Lett.* **2000**, *327*, 181.
[30] L. Romaner, G. Heimel, E. Zojer, *Phys. Rev. B* **2008**, *77*, 045113.
[31] E. Zojer, T. C. Taucher, O. T. Hofmann, *Adv. Mater. Interfaces* **2019**, *6*, 1900581.
[32] T. Schultz, T. Lenz, N. Kotadiya, G. Heimel, G. Glasser, R. Berger, P. W. M. Blom, P. Amsalem, D. M. de Leeuw, N. Koch, *Adv. Mater. Interfaces* **2017**, *4*, 1700324.
[33] S. Blumstengel, H. Glowatzki, S. Sadofev, N. Koch, S. Kowarik, J. P. Rabe, F. Henneberger, *Phys. Chem. Chem. Phys.* **2010**, *12*, 11642.
[34] F. Piersimoni, R. Schlesinger, J. Benduhn, D. Spoltore, S. Reiter, I. Lange, N. Koch, K. Vandewal, D. Neher, *J. Phys. Chem. Lett.* **2015**, *6*, 500.
[35] C. Edder, J. M. J. Fréchet, *Org. Lett.* **2003**, *5*, 1879.
[36] N. Kakiuchi, H. Furusho, N. Otani, T. Minami, T. Okauchi, *EP 1 882 694 A1* **2008**.
[37] L. Pasquali, A. DeLuisa, S. Nannarone, *AIP Conf. Proc.* **2004**, *705*, 1142.
[38] S. Nannarone, F. Borgatti, A. DeLuisa, B. P. Doyle, G. C. Gazzadi, A. Giglia, P. Finetti, N. Mahne, L. Pasquali, M. Pedio, G. Selvaggi, G. Naletto, M. G. Pelizzo, G. Tondello, *AIP Conf. Proc.* **2004**, *705*, 450.
[39] K. Hermann, L. G. M. Pettersson, M. E. Casida, C. Daul, A. Goursot, A. Koester, E. Proynov, A. St-Amant, D. R. Salahub, StoBe-deMon version 3.0 **2007**.
[40] A. Yassar, G. Horowitz, P. Valat, V. Wintgens, M. Hmyene, F. Deloffre, P. Srivastava, P. Lang, F. Garnier, *J. Phys. Chem.* **1995**, *99*, 9155.
[41] H. Li, P. Winget, J.-L. Bredas, *Adv. Mater.* **2012**, *24*, 687.